



## OPEN ACCESS

## EDITED BY

Ana Luisa Garcia-Oliveira,  
The International Maize and Wheat  
Improvement Center (CIMMYT), Kenya

## REVIEWED BY

Xi Zhang,  
Dalhousie University, Canada  
Evan Forsythe,  
Colorado State University, United States  
Hakim Manghwar,  
Lushan Botanical Garden (CAS), China

## \*CORRESPONDENCE

Meng Li,  
mengli.kib@gmail.com

## SPECIALTY SECTION

This article was submitted to Plant  
Genomics,  
a section of the journal  
Frontiers in Genetics

RECEIVED 09 August 2022

ACCEPTED 30 September 2022

PUBLISHED 13 October 2022

## CITATION

Zhao J, Pu X, Li W and Li M (2022),  
Characterization and evolutionary  
diversification of the phospholipase D  
gene family in mosses.  
*Front. Genet.* 13:1015393.  
doi: 10.3389/fgene.2022.1015393

## COPYRIGHT

© 2022 Zhao, Pu, Li and Li. This is an  
open-access article distributed under  
the terms of the [Creative Commons  
Attribution License \(CC BY\)](#). The use,  
distribution or reproduction in other  
forums is permitted, provided the  
original author(s) and the copyright  
owner(s) are credited and that the  
original publication in this journal is  
cited, in accordance with accepted  
academic practice. No use, distribution  
or reproduction is permitted which does  
not comply with these terms.

# Characterization and evolutionary diversification of the phospholipase D gene family in mosses

Jinjie Zhao<sup>1</sup>, Xinyuan Pu<sup>1</sup>, Wenfei Li<sup>1</sup> and Meng Li<sup>2\*</sup>

<sup>1</sup>State Key Laboratory for Conservation and Utilization of Bio-Resources in Yunnan, Research Center for Perennial Rice Engineering and Technology of Yunnan, School of Agriculture, Yunnan University, Kunming, Yunnan, China, <sup>2</sup>Yunnan Academy of Tobacco Science, Kunming, Yunnan, China

Plant phospholipase D (PLD) exerts important roles in various biological processes, such as intracellular signaling and morphological development. Our knowledge about early land plant *PLDs* is still underdeveloped. In this study, we identified 84 *PLD* genes in six mosses, i.e., *Physcomitrella patens*, *Ceratodon purpureus*, *Fontinalis antipyretica*, *Pleurozium schreberi*, *Sphagnum magellanicum*, and *Sphagnum fallax*. These *PLDs* were classified into four clades (I–IV). We showed that *PLD* underwent rapid expansion in mosses. A total of six conserved domains and two core HKD motifs were detected. Structure analysis uncovered that the moss *PLDs* from within a clade generally exhibited similar exon-intron organization. *Cis*-elements prediction and expression analyses indicated that *P. patens* *PLDs* had key roles in stress responsiveness and plant development. Particularly, about half of the *P. patens* *PLDs* (e.g., *PpPLD1*, *PpPLD2*, and *PpPLD5*) were differentially expressed under biotic and abiotic stresses. We also determined the expression pattern of *P. patens* *PLD* genes in various tissues and at different stages of development. Although the moss, clubmoss, liverwort, and fern *PLDs* evolved largely under functional constraints, we found episodic positive selection in the moss *PLDs*, e.g., *C. purpureus* *PLD2* and *P. patens* *PLD11*. We infer that the evolutionary force acting on the *PLDs* may have facilitated moss colonization of land. Our work provides valuable insights into the diversification of moss *PLD* genes, and can be used for future studies of their functions.

## KEYWORDS

bryophytes, gene structure, lineage-specific gene duplication, molecular evolution, three-dimensional structure

## Introduction

Phospholipase D (PLD) is a class of enzymes belonging to the phospholipase superfamily (Wang, 2000; Jang et al., 2012). The hydrolysis of phospholipids into phosphatidic acid has a wide impact on biological processes, such as, intracellular signaling, lipid remodeling, cytoskeletal reorganization, and vesicular trafficking (Zhang et al., 2010). In plants, PLDs are implicated in resistance to abiotic and biotic

stresses (Pinosa et al., 2013; Ufer et al., 2017), growth (Hong et al., 2009), and seed development (Ryu et al., 1996). Based on the presence of either the calcium/lipid-binding (C2) or the phox/pleckstrin homology (PX/PH) domains, PLDs can be divided into C2 and PX/PH PLDs. The C2 domain regulates Ca<sup>2+</sup>-dependent activity (Kopka et al., 1998), while the PX/PH domains target phosphoinositide-rich membrane compartments (Hong et al., 2017). In addition to C2 and PX/PH PLDs, there is another type of phospholipase referred to as signal peptide (SP) PLD, which lacks the C2 and PX/PH domains but carrying an N-terminal signal peptide (Selvy et al., 2011). With the help of a signal peptide, SP PLD is secreted into the extracellular spaces to hydrolyze its substrates (Qu et al., 2021). In rice, SP PLD expression was downregulated during the entire reproductive stage (Singh et al., 2012).

The *Arabidopsis thaliana* PLDs include six subfamilies, i.e.,  $\alpha$ ,  $\beta$ ,  $\gamma$ ,  $\delta$ ,  $\epsilon$ , and  $\zeta$  (Wang, 2005). The calcium/lipid-binding C2 domain is common in PLD $\alpha$ ,  $\beta$ ,  $\gamma$ ,  $\delta$ , and  $\epsilon$ , and the PX/PH domains are prevalent in PLD $\zeta$ . The  $\alpha$  subfamily has the most redundant PLDs in both *A. thaliana* (three PLD $\alpha$ s) and *Oryza sativa* (eight PLD $\alpha$ s), and this may also be true in other seed plants (Bourtsala et al., 2017). Previous studies indicate that PLD $\alpha$  is involved in response to diverse stresses, including drought, freezing, physical injury, and high salinity (Mane et al., 2007; Hong et al., 2008; Kargiotidou et al., 2010; Bourtsala et al., 2017; Ufer et al., 2017). It is also suggested that PLDs from distinct subfamilies are active at different steps of a single biological process. For instance, PLD $\alpha$  and PLD $\delta$  are activated at different time points in cotton (*Gossypium hirsutum*) wound signaling (Bourtsala et al., 2017). In addition to those of *A. thaliana* and *O. sativa*, PLDs in various angiosperms have been investigated. For example, 10 and 16 PLDs were found in the genome of pineapple (*Ananas comosus*) and potato (*Solanum tuberosum*), respectively (Hong et al., 2017; Li et al., 2021). When treated with hexaldehyde, the expression of PLD2 in pineapple fruit was upregulated (Hong et al., 2017). A total of 17 and 11 PLDs were identified in poplar (*Populus trichocarpa*), and grape (*Vitis vinifera*), respectively. In poplar, a fast expansion constituted by five species-specific PLD gene duplications was reported (Liu et al., 2010).

Mosses are different from angiosperms in many aspects, such as morphology (Beerling et al., 2001), secondary metabolism (Pichersky and Gang, 2000), and life cycle (Boyce, 2008). Knowledge about PLDs in bryophytes is still limited, although several moss genomes have been sequenced ([https://www.plabipd.de/plant\\_genomes\\_pn.ep](https://www.plabipd.de/plant_genomes_pn.ep)). As such, in this study we performed a genome-wide identification of PLDs in six moss genomes, i.e., *Physcomitrella patens*, *Ceratodon purpureus*, *Fontinalis antipyretica*, *Pleurozium schreberi*, *Sphagnum magellanicum*, and *Sphagnum fallax*. The phylogenetic and molecular evolution of PLDs in mosses were thoroughly explored to elucidate the evolutionary divergence of the moss PLD gene family. We also considered conserved sequence

characteristics and expression patterns. This provides foundational knowledge for understanding the diversification of moss PLD genes.

## Materials and methods

### Data sources and identification of PLD homologs

The proteome and genome files of *P. patens* (v3.3), *C. purpureus* (GG1, v1.1), *Ceratopteris richardii* (v2.1), *Marchantia polymorpha* (v3.1), and *Selaginella moellendorffii* (v1.0) were downloaded from the Joint Genome Institute (DOE-JGI, <https://phytozome-next.jgi.doe.gov/>). The sequence data of *Azolla filiculoides* and *Salvinia cucullata* were obtained from Fernbase (<https://www.fernbase.org/>) (Li et al., 2018). The genome data of *F. antipyretica* was acquired from GigaDB (<http://gigadb.org/dataset/100748>) (Yu et al., 2020). The proteome of *P. schreberi* was retrieved from GitHub project webpage ([https://github.com/PycnopodiaD/Pleurozium\\_schreberi\\_annotated\\_genome\\_files](https://github.com/PycnopodiaD/Pleurozium_schreberi_annotated_genome_files)) (Pederson et al., 2019). Using *A. thaliana* and *O. sativa* PLD sequences as queries, BLASTP (Camacho et al., 2009) and hmmsearch (<http://hmmer.org/>) were employed to search against the collected protein sequence datasets. For *S. magellanicum* and *S. fallax*, online BLASTP searches were performed at the phytozome website (DOE-JGI, <https://phytozome-next.jgi.doe.gov/blast-search>). Additional BLASTP searches were performed on the NCBI nonredundant (nr) database to obtain as many PLD candidates as possible. A candidate was considered a PLD when either the phospholipase D domain or the phospholipase D C terminal domain was detected.

### Sequence alignment and phylogenetic tree reconstruction

The PLD protein sequences were aligned in MAFFT (v7.450), using the strategy determined by '--auto' option (Katoh and Standley, 2013). Poorly aligned positions were eliminated using trimAl (v1.4), by allowing a maximum of 30% gaps per sequence (Capella-Gutierrez et al., 2009). IQ-TREE (v1.5.4) with options "--nt AUTO -m TEST -bb 1000 -alrt 1000" was used to identify the best-fit amino acid substitution model for the PLD sequence alignment (LG + I + G was selected according to the BIC score), and then to reconstruct the maximum likelihood phylogenetic tree (Nguyen et al., 2015). Bootstrap values were estimated by 1000 ultrafast bootstrap and SH-like approximate likelihood ratio tests. Bayesian analysis was performed using MrBayes (v3.2.7) (Ronquist et al., 2012). Two independent runs with eight chains each were calculated simultaneously and iteratively until the average standard deviation of the split

frequencies was below 0.05 (The Markov chain Monte Carlo chain was run for more than 400 million generations). Trees were sampled every 100 generations. After discarding the first 25% of sampled trees, the posterior probability values were produced. The final tree was visualized in Figtree (v1.4.4, <http://tree.bio.ed.ac.uk/software/figtree/>).

## Detection of domains, motifs, and signal peptide sequences

Identification of conserved domains was performed by searching the Pfam (Finn et al., 2013) and SMART (Letunic et al., 2020) databases. Conserved motifs were determined using the MEME/MAST software (Bailey and Gribskov, 1998). SignalP (<http://www.cbs.dtu.dk/services/SignalP-4.1/>) (Nielsen, 2017) was used to predict the signal peptide sequences.

## Gene structure analyses

Gene structure information was retrieved from genome annotation files or GenBank. For genes with two or more transcripts, the exon number referred to the average number of exons. Group differences of exon number were tested by ANOVA followed by a pairwise *t* test with Bonferroni correction (Fisher, 1992). All statistical analyses were performed using R (v3.6.2, <https://www.r-project.org/>) software.

## Analysis of *cis*-regulatory elements in the promoter region of *PpPLDs*

The 2-kb promoter sequences upstream of the *PpPLDs* extracted from the *P. patens* genome were submitted to the PlantCARE database (<http://bioinformatics.psb.ugent.be/webtools/plantcare/html/>) to perform the *cis*-acting element analysis. The identified *cis*-elements were displayed using a custom script written in the R programming language (v3.6.2, <https://www.r-project.org/>).

## Expression analyses

RNA-seq data used for expression analyses were retrieved from the NCBI Sequence Read Archive (SRA) database: *P. patens*: PRJDB6633; *C. purpureus*: PRJNA622159—PRJNA622174, and PRJNA622207; *F. antipyretica*: PRJEB21674; *C. richardii*: PRJNA681601; *A. filiculoides*: PRJNA264391 and PRJEB25913; *S. cucullate*: PRJNA430459; *M. polymorpha*: PRJNA554398, PRJDB6783, and PRJNA350270. Reads were mapped to the reference coding sequences by using kallisto (v0.46.1) (Bray et al.,

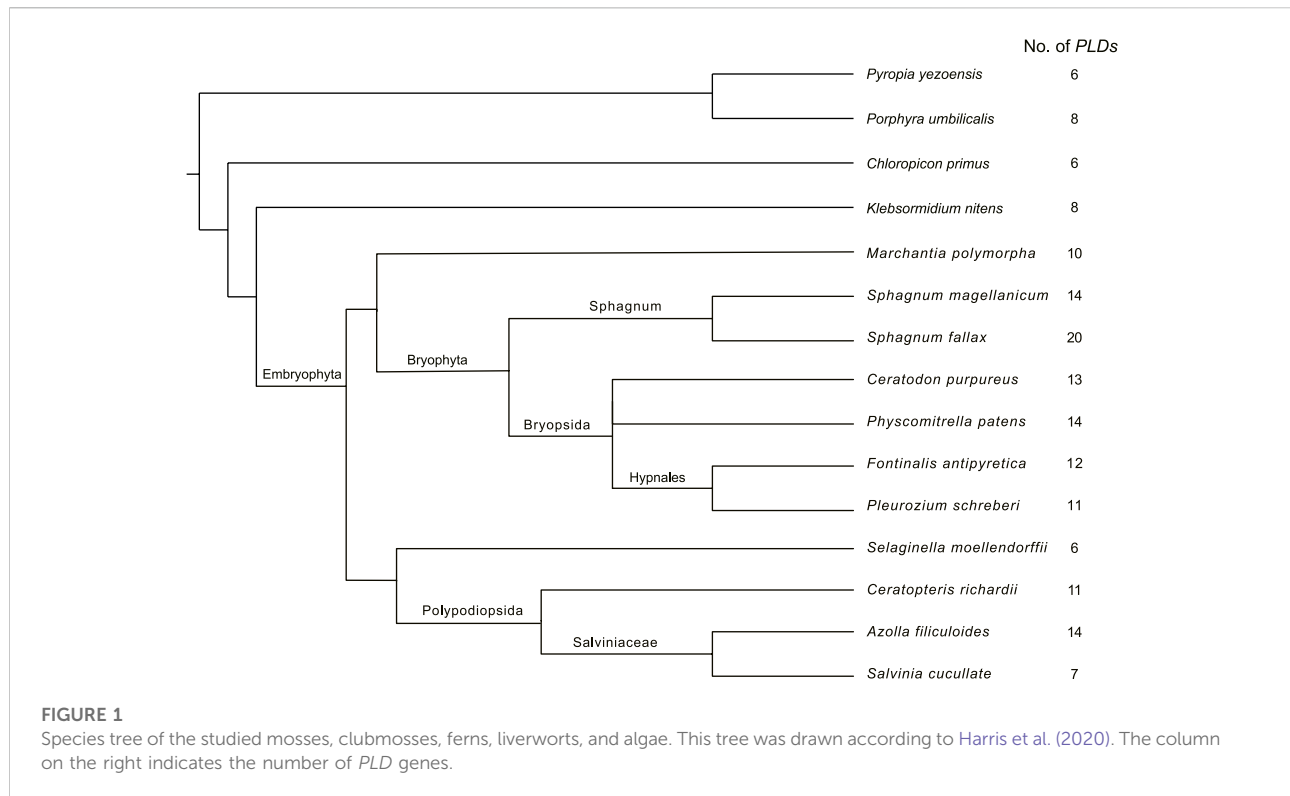
2016). Expression levels were evaluated by transcripts per million (TPM). If more than one transcript were present, the average TPM would be calculated for following analyses. Expression data for *S. moellendorffii* were extracted from the eFP Browser (<http://bar.utoronto.ca/>) of Selaginella. No RNA-seq data were publicly available for *S. fallax*, *S. magellanicum*, and *P. schreberi*. For *P. patens* *PLDs*, expression profiles of different tissues, including spores, caulonema, chloronema, protoplast, rhizoids, gametophore, archegonia, and sporophytes from the S1, S2, S3, and M stages, were collected from the Physcomitrella eFP Browser (Ortiz-Ramirez et al., 2016). The *P. patens* RNA-seq data (PRJNA611083) generated after inoculation of fungal pathogen (*Botrytis cinerea*) were downloaded to analyze biotic stress-induced expression of *PpPLDs*. The RNA-seq data (PRJNA596891) of *P. patens* plants grown under a salinity stress condition (200 mM NaCl) were used to examine abiotic stress-induced expression pattern.

## Molecular evolutionary analyses

The *PLD* coding sequences were aligned using the program “reportGapsAA2NT” implemented in MACSE (v2.05) (Ranwez et al., 2018). To avoid bias introduced by short sequences, 11 out of the identified 132 *PLDs* whose coding sequence length <900 bp (The average coding sequence length of the identified moss, clubmoss, fern, and liverwort *PLDs* is 2400 bp), e.g., *M. polymorpha* *PLDs* 8–10, were excluded from evolutionary pressure analyses. Molecular evolutionary analyses were applied to the SP *PLDs* separately, because they shared low sequence similarities to C2 and PX/PH *PLDs*. Positive and purifying selection were determined by the ratio of non-synonymous to synonymous nucleotide substitutions ( $\omega$ , also known as  $d_N/d_S$ ). The Fast, Unconstrained Bayesian Approximation (FUBAR) (Murrell et al., 2013), Mixed Effects Model of Evolution (MEME) (Murrell et al., 2012), Branch-Site Unrestricted Statistical Test for Episodic Diversification (BUSTED) (Murrell et al., 2015), and adaptive Branch-Site Random Effects Likelihood (aBSREL) (Smith et al., 2015) methods were run using the HyPhy software package (Kosakovsky Pond et al., 2020). Changes in selection intensity were estimated using the RELAX method (Wertheim et al., 2015). The branch-site model analysis was conducted using the CODEML program from the PAML package (v4.9j) (Yang, 2007).

## Three-dimensional structure prediction

AlphaFold v2.0 (Jumper et al., 2021) was used to predict the 3D structures for *PpPLD11*, with the resources and default parameters provided at the ColabFold website (<https://colab.research.google.com/github/sokrypton/ColabFold/blob/main/AlphaFold2.ipynb>). To perform homology modeling, the protein sequence of



PpPLD11 was analyzed by searching the SWISS-MODEL database (<http://swissmodel.expasy.org/>) (Waterhouse et al., 2018). The quality of the predicted 3D structure was assessed using SAVES (<https://saves.mbi.ucla.edu/>). Pymol software (<https://pymol.org/>) was applied to visualize the 3D structure.

## Results

### Identification and annotation of PLDs in available moss genomes

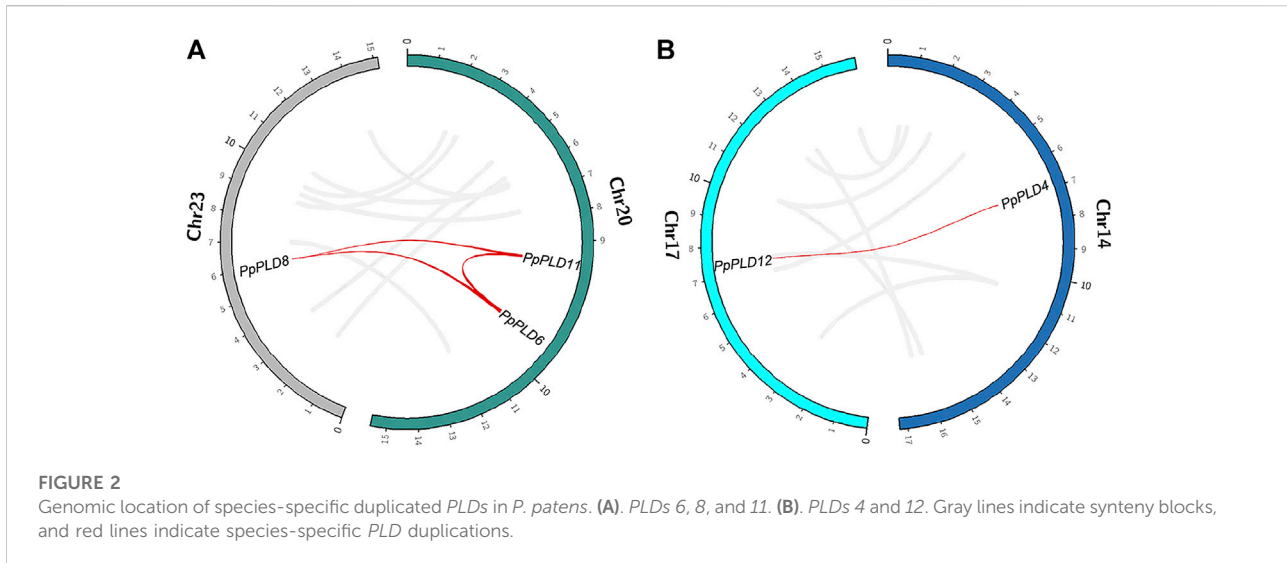
To gain insights into the distribution of PLD in mosses, we mined homologous PLD genes from the genomes and proteomes of six bryophytes, *P. patens*, *C. purpureus*, *F. antipyretica*, *P. schreberi*, *S. magellanicum*, and *S. fallax*. A total of 14, 13, 12, 11, 14, and 20 PLDs were identified in these species, respectively (Supplementary Table S1). Further, we investigated the presence of PLDs in another five early land plant species, categorized as clubmosses (*S. moellendorffii*), ferns (*C. richardii*, *A. filiculoides*, and *S. cucullate*), and liverworts (*M. polymorpha*). In total, 132 PLD homologous sequences were identified (Supplementary Table S1). As shown in Figure 1, the number of PLD genes varies widely between species, ranging from six (*S. moellendorffii*) to 20 (*S. fallax*). These PLD homologs were named according to a common nomenclature consisting of the first letters of both

the genus (upper case) and the species (lower case), followed by the PLD identifier and a number arranged by its order of domain conservation.

We further analyzed the genomic location of the identified PLDs. In the *P. patens* genome, 12 of 14 PLDs were mapped separately onto 12 chromosomes (chromosomes 2, 3, 7, 8, 10, 12–14, 17, 18, 22, and 23. Figures 2A,B, and Supplementary Figure S1). On chromosome 20, PpPLD6 was located nearly adjacent to PpPLD11. Similar patterns were also observed in *S. magellanicum*, *S. fallax*, *C. richardii*, and *C. purpureus* (Supplementary Figure S1). Such co-locations were not found for PLDs in *F. antipyretica*, *P. schreberi*, *S. moellendorffii*, *A. filiculoides*, *S. cucullate*, and *M. polymorpha*, partly because genomes of these species were not fully assembled.

### Origin and diversification of the moss PLDs

Phylogenetic analyses were carried out on the above-mentioned moss, clubmoss, fern, and liverwort PLDs, together with another 55 from *A. thaliana*, *O. sativa*, *Thuja plicata*, and red and green algae to explore the origin of the moss PLDs. The phylogenetic trees reconstructed using the maximum likelihood and Bayesian methods shared a similar topology. As displayed in Figure 3; Supplementary Figure S2, the green plant PLDs are classified into four clades (I–IV). The C2 PLDs clustered within clades I and II, and PX/PH PLDs



clustered within clade III. The SP *PLDs* were located in clade IV. For *A. thaliana* and *O. sativa*, the  $\alpha$  and  $\epsilon$  *PLDs* were grouped into clade I. The  $\beta$ ,  $\gamma$ , and  $\delta$  *PLDs* were grouped into clade II. The  $\zeta$  and  $\phi$  *PLDs* were clustered in clades III and IV, respectively.

According to the phylogeny, the most ancient *PLDs* in clade I (*PLD* $\alpha$ s and *PLD* $\epsilon$ s) could be found in three red algae species *Pyropia yezoensis*, *Porphyridium purpureum*, and *Porphyra umbilicalis*. For clade II ( $\beta$ ,  $\gamma$ , and  $\delta$ ) *PLDs*, orthologs from *Klebsormidium nitens* and *Chara braunii*, two charophytic algae very closely related to land plants, were placed on the root. Similarly, the most ancient orthologs of clade III *PLDs* (*PLD* $\zeta$ s) came from *K. nitens* and *C. braunii*. For clade IV *PLDs* (*PLD* $\phi$ s), we identified one homolog from *Chloropicon primus*, a tiny marine green alga, and two homologs from *P. yezoensis* and *P. purpureum*.

Within each *PLD* clade, the *PLDs* of peatmosses and true mosses (Bryopsida) were clustered tightly together, forming five separate sub-clades (A–E) (Figure 3), consistent with their taxonomic classification. It was noteworthy that three of these five moss sub-clades (i.e., sub-clades A, C, and D) could be further divided into two groups, each comprising *PLDs* from *S. magellanicum*, *S. fallax*, *C. purpureus*, *P. patens*, *F. antipyretica*, and *P. schreberi*. Furthermore, phylogenetic analysis suggested that the *PLD* family underwent four species-specific gene duplications in mosses, that is, *CpPLDs* 2 and 3; *PpPLDs* 6, 8 and 11; *PpPLDs* 4 and 12; *SfPLDs* 10, 13–16, and 20 (Figure 3).

## Conserved domains and motifs in the moss *PLDs*

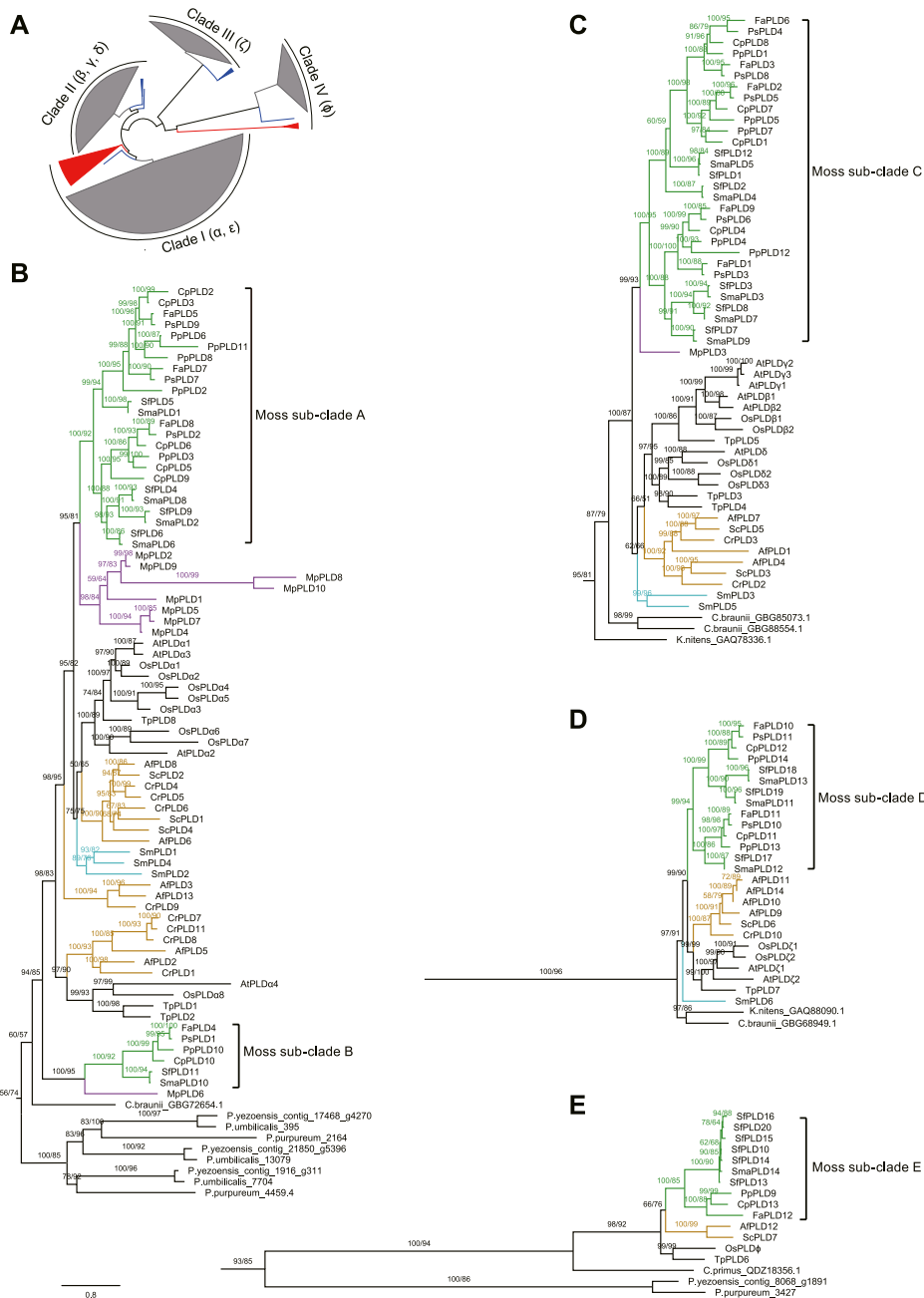
The phospholipase D, phospholipase D C terminal, C2, and PX/PH domains commonly reported in angiosperm *PLDs* were identified in moss *PLDs* (Supplementary Table S2; Supplementary

Figure S3). In mosses, clubmosses, ferns, and liverworts, most of the obtained *PLDs* contained the phospholipase D domain, except for *MpPLDs* 8–10 and *AfPLD14* (Supplementary Table S2). The phospholipase D C terminal and C2 domain were found in moss *PLDs* within clades I and II ( $\alpha$ ,  $\beta$ ,  $\gamma$ ,  $\epsilon$ , and  $\delta$  *PLDs*), with a few exceptions. For example, the C2 domain was missing in *PpPLD11*, *PpPLD12*, *PsPLDs* 1–4 and 8, *FaPLDs* 4 and 6, and *CpPLD10*. The PX/PH domains were specific to clade III *PLDs* (*PLD* $\zeta$ s) (Figure 4). However, in moss clade III *PLDs* (*PLD* $\zeta$ s), *FaPLD10* did not contain the PX domain, and *SfPLD18* and *SmaPLD13* did not have the PH domain. In addition, signal peptide sequences were observed in the moss clade IV ( $\phi$ ) *PLDs* (*SfPLDs* 10, 14, and 20, *SmaPLD14*, *FaPLD12*, and *PpPLD9*).

The HKD (H×K××××D) motifs are also frequently noted characteristics in angiosperm *PLDs* (Elias et al., 2002). Using the MEME/MAST software (Bailey and Gribskov, 1998), we found that HKD1 and HKD2 motifs were present in most of the moss *PLDs*, with a few exceptions (Figure 4; Supplementary Figure S3; Supplementary Table S2). For instance, the HKD1 motif was absent in *PpPLD12*, *PsPLDs* 1 and 2, *FaPLD12*, and *SfPLDs* 14, 15, and 20. A total of 18 moss *PLDs* lacked the HKD2 motif, e.g., *CpPLD13*, *PpPLD9*, and *SmaPLD14*.

## Gene structure analyses in the moss *PLDs*

Given that the diversity of gene structure is important for the evolution of a gene family (Liu et al., 2009), the exon-intron structures of moss *PLDs* were analyzed. As shown in Supplementary Figure S4, *PLDs* within a clade generally share similar exon-intron structures, in a manner roughly consistent with their phylogenetic relationships. For instance, both *SfPLD4* and *SmaPLD8* contained five exons, with almost identical exon-intron structures. In these two genes, the first



**FIGURE 3**

Phylogenetic unrooted tree of PLDs from mosses, clubmosses, liverworts, ferns, angiosperms, and algae. Because it was not clear when the C2, PX/PH, and SP PLD subfamilies diverged (perhaps long before the emergence of red algae), no outgroup was used for this tree. **(A)**: A simplified overview of the entire phylogenetic tree with clades I, II, III, and IV collapsed. Blocks colored in grey, red, and blue represent PLDs of land plants (mosses, clubmosses, liverworts, ferns, and angiosperms) and red and green algae, respectively. **(B–E)**: Phylogenetic topologies within clades I, II, III, and IV, respectively. The original phylogenetic tree is displayed in Supplementary Figure S2. The sequence alignment used was provided in supplementary data sheet 1. Above branches are bootstrap supports from maximum likelihood and Bayesian analyses, respectively. The bootstrap value below 50% is not shown. The green, purple, orange, and cyan color on the branches refer to mosses, liverworts, ferns, and clubmosses, respectively. Scale bar represents substitution numbers per amino-acid site for **(B–E)**. The abbreviations used are as follows: Pp, *P. patens*; Cp, *C. purpureus*; Fa, *F. antipyretica*; Ps, *P. schreberi*; Sma, *S. magellanicum*; Sf, *S. fallax*; Sm, *S. moellendorffii*; Cr, *C. richardii*; Af, *A. filiculoides*; Sc, *S. cucullate*; Mp, *M. polymorpha*; At, *A. thaliana*; Os, *O. sativa*; Tp, *T. pilcata*.

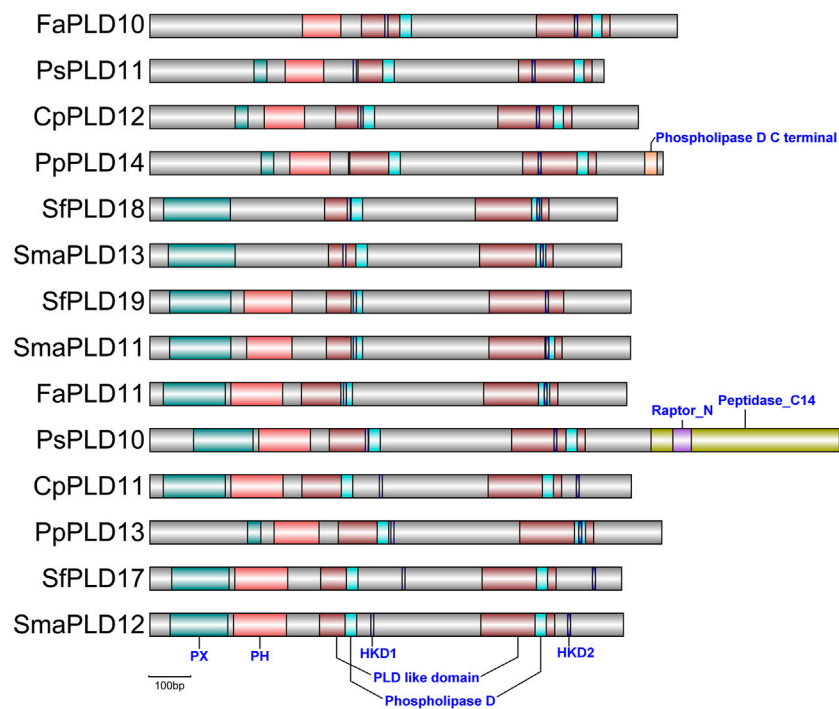


**FIGURE 4**

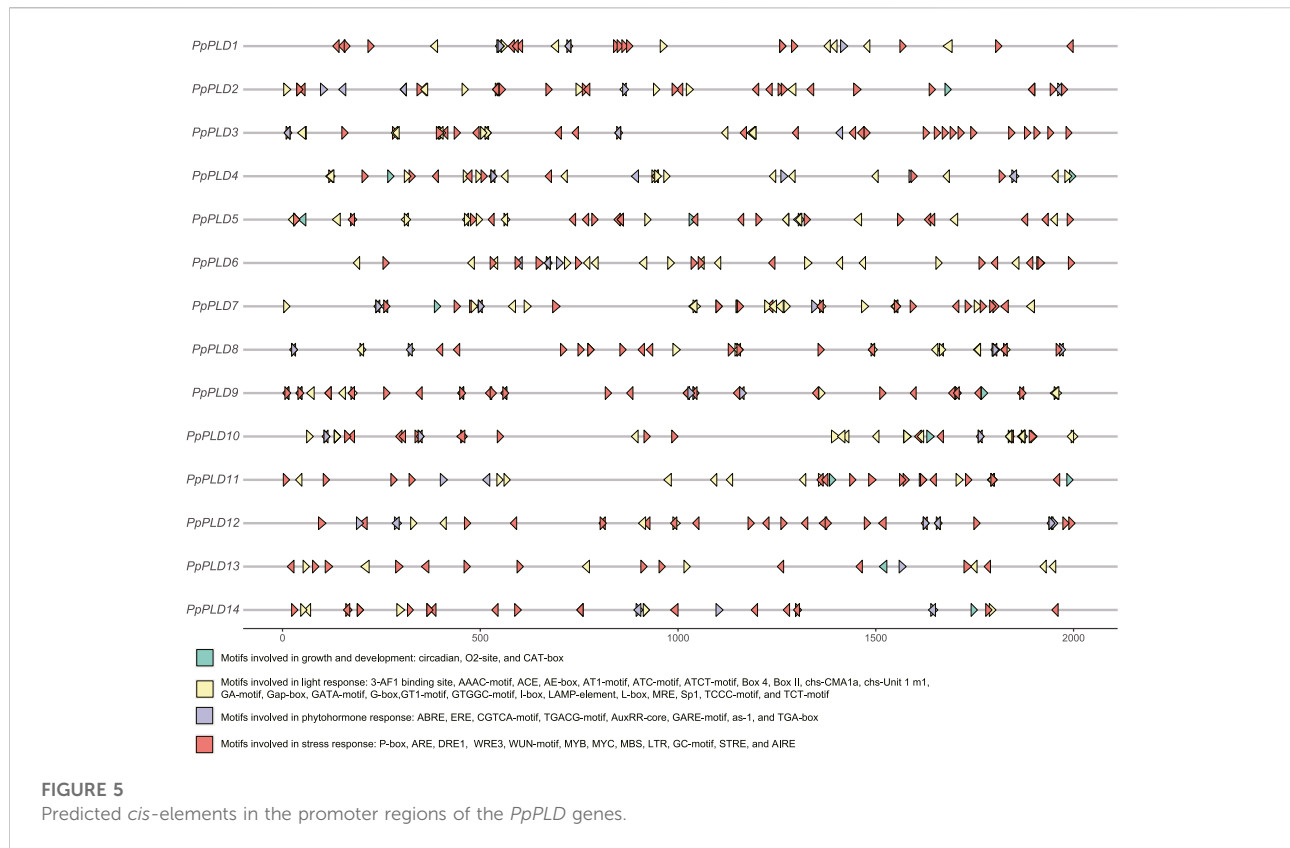
Conserved domains and motifs observed in moss clade III (PX/PH) *PLDs*. The full conserved domains and motifs detected in all *PLDs* were displayed in Supplementary Table S2 due to page limitation. The *PLDs* are ordered according to the phylogenetic tree displayed in Figure 3. The grey bars indicate the *PLD* protein sequences. The phospholipase D (Pfam accession number: PF00614) and *PLD* like domains (Pfam accession number: PF13091/PF13918) are indispensable for hydrolyzing phosphatidylcholine into phosphatidic acid. The phospholipase D C terminal (Pfam accession number: PF12357) can bind to calcium. The PX domain (Pfam accession number: PF00787) contains a pbox consensus sequence. The PH (Pfam accession number: PF00169) is a pleckstrin homology domain approximately 120 amino acids in length. The HKD1 and HKD2 motifs contain the core sequence "HxKxxxxD".

and second exons were about 600 and 150 bp, respectively, with the first intron measuring about 170 bp. Another representative case was the pair of *SfPLD11* and *SmaPLD10*, both of which possessed three exons, and shared highly similar gene structures. When the *PLDs* of clubmosses, ferns, and liverworts were taken into consideration, the clade II ( $\beta$ ,  $\gamma$ , and  $\delta$ ) *PLDs* had the largest average number of exons, approximately 9.6 per gene (Supplementary Figure S5), significantly more than those of clades I and IV ( $\alpha$ ,  $\epsilon$ , and  $\phi$  *PLDs*, 3.8 and 6 average exons per gene, respectively). Interestingly, PX/PH *PLDs* ( $\zeta$ , clade III) of peatmosses and true mosses had an average of 2.6 exons per gene, significantly fewer than those of ferns, clubmosses and *K. nitens* (on average 16.9, 20, and 16 exons per gene, respectively), suggesting intron loss in the moss PX/PH ( $\zeta$ ) *PLDs*.

### Examination of *cis*-elements in promoters of *P. patens* *PLD* genes

*Cis*-elements of the promoter region can regulate gene transcription and function. As shown in Figure 5, the *cis*-acting elements observed in *PpPLD* gene promoters can be

divided into four general groups, i.e., stress-, light-, phytohormone-, and growth and development-correlated motifs. Five stress associated (drought, salt, low-temperature, wound, and anaerobic) responsive elements consisting of P-box, ARE, DRE1, WRE3, WUN-motif, MYB, MYC, MBS, LTR, GC-motif, STRE, and AIRE, constituted the most redundant *cis*-elements in *PpPLD* genes. Specifically, several stress related elements were extensively dispersed in *PpPLDs* 3 and 9. The light response involved motifs were the second-most enriched *cis*-elements in the *PpPLD* gene promoters. The identified light responsive elements included 3-AF1 binding site, AAAC-motif, ACE, AE-box, AT1-motif, ATC-motif, ATCT-motif, Box 4, Box II, chs-CMA1a, chs-Unit 1 m1, GA-motif, Gap-box, GATA-motif, G-box, GT1-motif, GTGGC-motif, I-box, LAMP-element, L-box, MRE, Sp1, TCCC-motif, and TCT-motif. Additionally, we found phytohormone-correlated motifs, including ABRE, ERE, CGTCA-motif, TGACG-motif, AuxRR-core, GARE-motif, as-1, and TGA-box. The plant growth and development related motifs were comprised of circadian (involved in circadian regulatory), O2-site (associated with zein



metabolism regulation), and CAT-box (related to meristem expression).

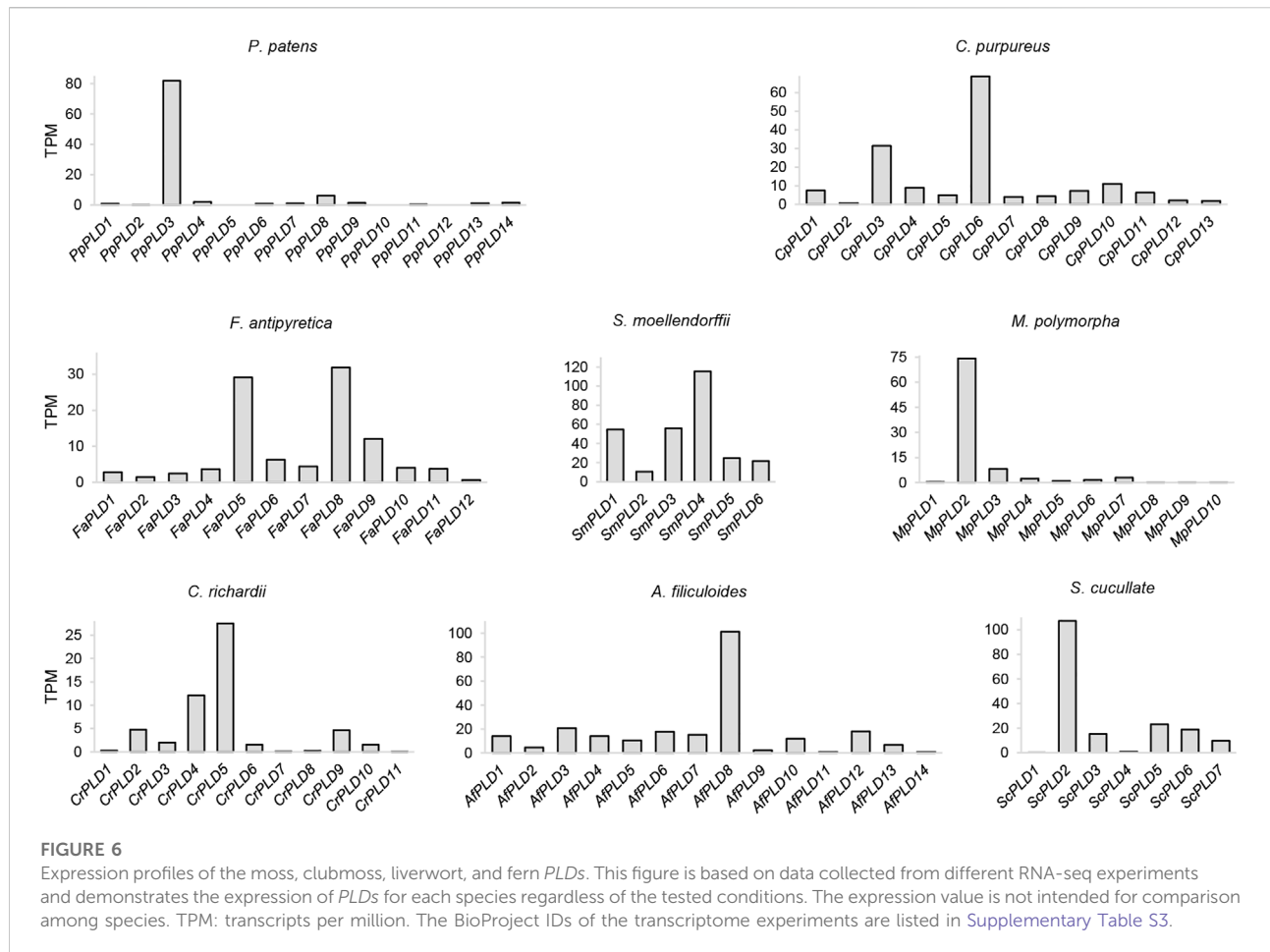
## Expression profiles of the moss *PLD* genes

The expression profile of a gene can provide useful information about its molecular function (Brown et al., 2005; Hansen et al., 2014). To analyze the transcriptional activity of the *PLDs*, we performed expression analyses. Publicly available RNA-seq data were found for *P. patens*, *C. purpureus*, *F. antipyretica*, *C. richardii*, *A. filiculoides*, *S. cucullata*, and *M. polymorpha* (Supplementary Table S3). For each of these species, an average of 165.25 GB of transcriptome data were collected. The expression level was estimated by TPM. As a result, most of the investigated moss, clubmoss, fern, and liverwort *PLDs* were expressed under certain conditions (Figure 6 and Supplementary Table S4). For instance, 11 of 14 *P. patens PLDs* were expressed; among these, *PpPLD3* was the most highly expressed (TPM = 81.88), suggesting it had a critical function in these experimental studies. Additionally, of the tested plants, in species other than *F. antipyretica* and *A. filiculoides*, both the highest and lowest expressed *PLDs* were found in clade I (*PLD $\alpha$* s and *PLD $\epsilon$* s). These results suggested that clade I *PLDs* maintained differentiated functions in the tested conditions.

## Analysis of *PLD* expression profiles in different tissues of *P. patens*

Tissue-specific expression profiles of *PpPLD* genes were examined in 11 various tissues, including caulonema, chloronema, protoplast, rhizoids, gametophore, archegonia, spores, and four developmental sporophytic stages, i.e., sporophyte S1, S2, S3, and M, using microarray expression data obtained from the Physcomitrella eFP Browser. In line with the RNA-seq results, *PpPLD3* was the top expressed in all tested tissues. For most *P. patens* tissues, the second highest expression levels were detected in *PpPLDs* 4, 7, and 8, and the lowest detectable expression level was found in *PpPLD5* (Figure 7A). The results also showed that *PpPLD* expression varied among tissues. For instance, *PpPLDs* 1 and 7 were preferentially expressed in protoplast; *PpPLDs* 2, 13, and 14 were most highly expressed in spores; Expression of *PpPLDs* 3, 4, and 10 were strongest in gametophore; expression of *PpPLDs* 5 and 6 were highest in archegonia; and *PpPLDs* 8 and 9 were most abundantly expressed in sporophyte M and chloronema, respectively. Additionally, in chloronema, expression of *PpPLDs* 2, 4, and 9 were moderate (the expression values ranged from 2000 to 3000). While in gametophore, moderate expression was observed in *PpPLDs* 1, 2, 10, and 13. In closely related tissues, such as caulonema and chloronema, several *PLD*





genes showed similar expression levels, e.g., *PpPLDs* 1, 3, 5, 7, and 8. During the sporophyte development, *PpPLD6* was highly expressed at the S1 stage and decreased after that, whereas expression of *PpPLD8* continued to increase after the S1 stage.

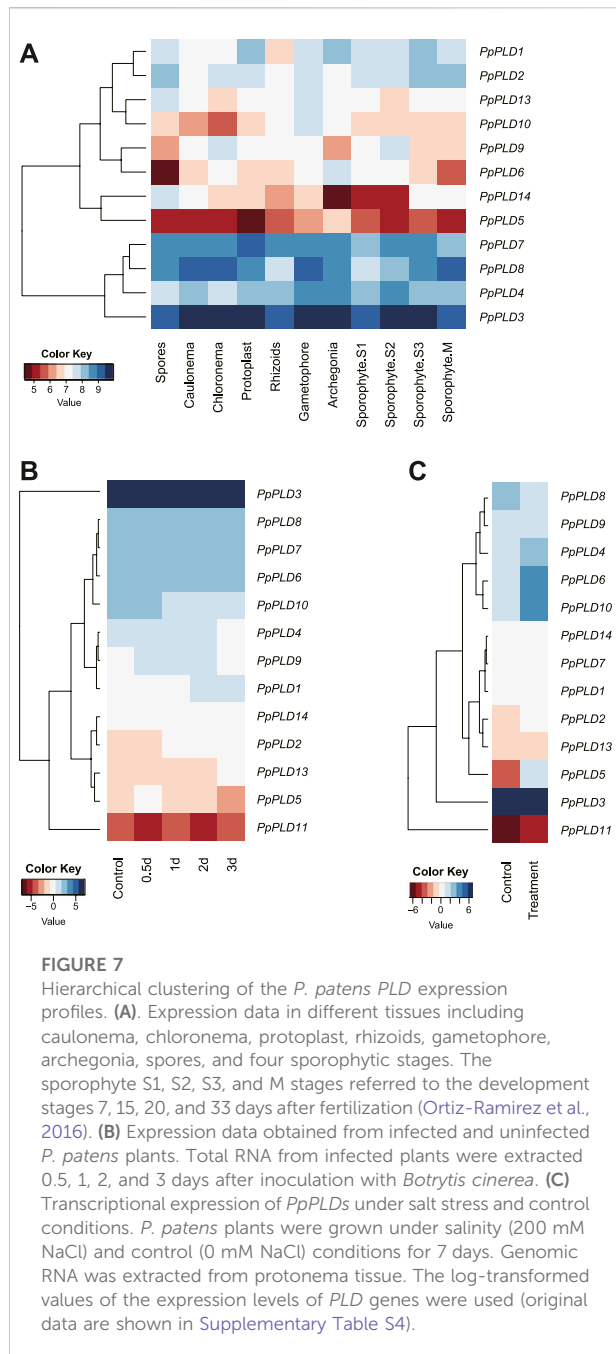
## Expression analyses of *PpPLDs* under biotic and abiotic stress conditions

The *cis*-element analysis suggested that *PpPLDs* played an important role in stress-responsive behavior. Therefore, we analyzed expression patterns of *PpPLD* genes under different biotic and abiotic stress conditions, including fungal pathogens and salt. For biotic stress, the RNA-seq data were generated at 0.5, 1, 2, and 3 days after infection of *Botrytis cinerea*. Expression of seven *PpPLDs* (i.e., *PpPLD1*, *PpPLD2*, *PpPLD5*, *PpPLD6*, *PpPLD10*, *PpPLD11*, and *PpPLD13*) were found to be significantly induced at least in one time point ( $\geq 1.5$ -fold change, [Figure 7B](#)). For instance, *PpPLD2* showed higher expression at 1 dpi (days after inoculation) (1.52 fold), 2 dpi (1.90 fold), and 3 dpi (1.71 fold). *PpPLD11* was upregulated at

0.5 dpi (2.67 fold), and downregulated at 2 dpi (2.00 fold). Under salinity stress, eight *PpPLDs* showed differential expression ( $\geq 1.5$ -fold change, [Figure 7C](#)). Upregulated genes included *PpPLD2* (1.71 fold), *PpPLD4* (2.38 fold), *PpPLD5* (27.55 fold), *PpPLD6* (3.47 fold), *PpPLD10* (5.53 fold), and *PpPLD11* (2.29 fold). *PpPLD7* and *PpPLD8* exhibited decreased expression (1.51 and 2.15-fold, respectively) when treated with NaCl.

## Selection pressures on the evolution of *PLD* genes of mosses

To unravel the molecular evolutionary mechanisms underlying the *PLDs* of mosses, clubmosses, ferns, and liverworts, the FUBAR method which can detect pervasive positive and negative selection at specific sites, alignment-wide (Murrell et al., 2013), was applied. We found no sites under positive selection, 193 sites from clades I–III ( $\alpha$ ,  $\beta$ ,  $\gamma$ ,  $\delta$ ,  $\epsilon$ , and  $\zeta$  *PLDs*), and 282 sites from clade IV (*PLD* $\phi$ s), with evidence of purifying selection at a posterior probability  $>0.9$



(Supplementary Table S5). Because selection is often transient rather than pervasive, we therefore restricted the analysis to moss PLDs, and adopted the MEME method (Murrell et al., 2012), which can identify individual sites that have experienced episodic positive selection under a proportion of branches. We found evidence of positive selection at 11 sites of the moss clades I–III ( $\alpha$ ,  $\beta$ ,  $\gamma$ ,  $\delta$ ,  $\epsilon$ , and  $\zeta$ ) PLDs, and at 16 sites of the moss clade IV PLDs (PLD $\phi$ s) ( $p < 0.05$ , Supplementary Table S5). The MEME method can detect selection at site-level, but cannot detect gene-wide selection. To detect gene-wide positive selection acting on

the moss PLDs, we used the BUSTED method which can test for positive selection on a subset of branches and at a proportion of sites (Murrell et al., 2015). As a result, about 0.90% sites of the moss PLDs from clades I–III ( $\alpha$ ,  $\beta$ ,  $\gamma$ ,  $\delta$ ,  $\epsilon$ , and  $\zeta$  PLDs) were found to be evolving with  $\omega > 1$  [likelihood ratio test statistic (LRT) = 34.56,  $p = 1.56 \times 10^{-8}$ , Table 1]. For the moss PLDs from clade IV (PLD $\phi$ s), 3.74% sites showed evidence of episodic positive selection ( $\omega = 8.48$ , LRT = 19.20,  $p = 3.38 \times 10^{-5}$ , Table 1). In addition to site-level and gene-wide selections, we also examined the branch-level episodic diversifying selection acting on the moss PLDs, using the aBSREL method (Smith et al., 2015). Episodic positive selections were identified on 3% sites of CpPLD2 ( $\omega_2 = 455.26$ , LRT = 21.57,  $p = 8.87 \times 10^{-4}$ ) and 22% sites of PpPLD11 ( $\omega_2 = 9.62$ , LRT = 17.07,  $p = 0.01$ , Supplementary Table S5). Since the aBSREL method does not report exactly which sites are under positive selection, we additionally performed the branch-site model analysis (by setting the CpPLD2 and PpPLD11 as foreground branches) using the CODEML program implemented in the PAML package. The likelihood ratio test comparing the modified model A (alternative model, fix\_omega = 0) with the corresponding null model (fix\_omega = 1) reached a significant level of  $p = 3.46 \times 10^{-7}$ . The alternative model reported that 24% sites of CpPLD2 and PpPLD11 had an estimate of  $\omega_2 = 7.44$ , among which 12 were statistically significant ( $p > 95\%$ ; 188T, 225K, 227P, 234E, 238L, 242C, 262K, 263F, 265Y, 334K, 366R, and 375Q of PpPLD11; Table 2). To ascertain if the selection pressures (both positive and purifying) observed on the moss PLDs were relaxed or intensified, we adopted the RELAX method which introduces an intensity parameter ( $k$ ).  $k > 1$  and  $k < 1$  indicate selective relaxation and intensification, respectively (Wertheim et al., 2015). Intensified selection was found in the moss sub-clade B PLDs comprising FaPLD4, PsPLD1, PpPLD10, CpPLD10, SfPLD11, and SmaPLD10 ( $k = 4.21$ ,  $p = 1.36 \times 10^{-6}$ , LRT = 23.34), and in the moss sub-clade D ( $\zeta$ ) PLDs ( $k = 1.23$ ,  $p = 0.01$ , LRT = 6.62). Additionally, we found evidence of relaxed selection in the moss sub-clade C PLDs ( $\beta$ ,  $\gamma$  and  $\delta$ ) ( $k = 0.75$ ,  $p < 0.05$ , LRT = 3.96).

### Three-dimensional structure prediction of PpPLD11

To gain insights into the function of the positively selected sites of PpPLD11, we predicted its crystal structure using AlphaFold (Figure 8). The per-residue confidence score (pLDDT, a value between 0 and 100) indicated that the PpPLD11 protein tertiary structure model had a high confidence. For homology modeling method, the protein sequence of *Arabidopsis* PLD $\alpha$ 1 (6 kz8.1A, which shared an identity of 56.9% with PpPLD11) was used as the template. The 3D structure of the PpPLD11 protein constructed by

**TABLE 1** The branch-site unrestricted statistical test for episodic diversification (BUSTED) results for moss *PLDs*.

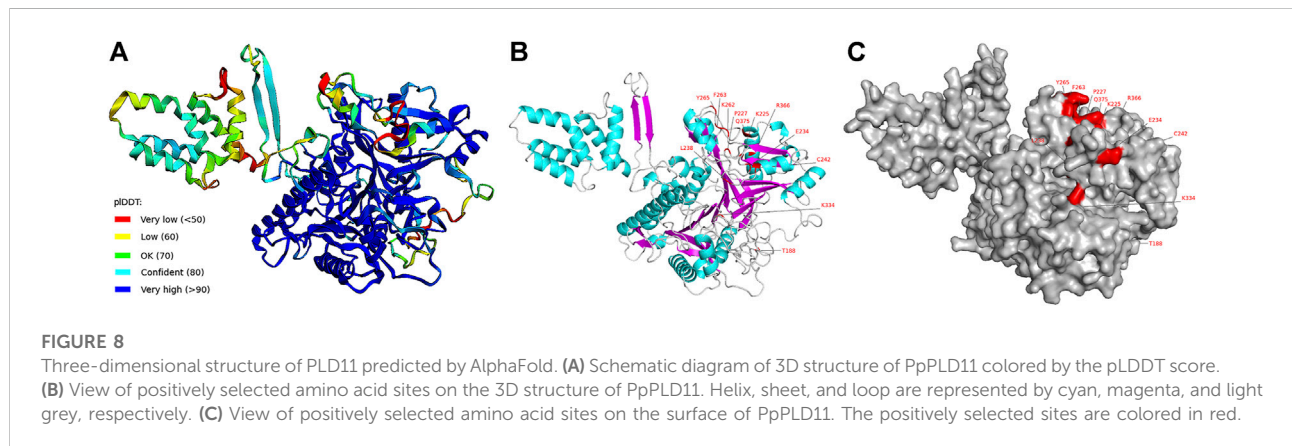
	Model	log L	LRT	Branch set	$\omega 1$ (proportion)	$\omega 2$ (proportion)	$\omega 3$ (proportion)
clades I–III ( $\alpha$ , $\beta$ , $\gamma$ , $\delta$ , $\epsilon$ , and $\zeta$ )	Constrained	−30023.40	34.56 $p = 1.56 \times 10^{-8}$	Background	0.01 (54.66%)	0.11 (43.43%)	104.02 (1.92%)
				Test	0.00 (65.04%)	0.08 (29.09%)	1.00 (5.87%)
	Unconstrained	−30006.20		Background	0.01 (56.13%)	0.11 (41.97%)	98.24 (1.90%)
				Test	0.00 (73.12%)	0.20 (25.98%)	11.94 (0.90%)
clade IV ( $\phi$ )	Constrained	−7920.12	19.20 $p = 3.38 \times 10^{-5}$	Background	0.03 (72.64%)	0.11 (15.36%)	1.00 (12.00%)
				Test	0.00 (32.16%)	0.08 (54.19%)	1.00 (13.65%)
	Unconstrained	−7910.52		Background	0.02 (68.71%)	0.13 (20.72%)	1.00 (10.57%)
				Test	0.00 (20.70%)	0.10 (75.56%)	8.48 (3.74%)

log L, log likelihood; LRT, likelihood ratio test statistic. Test branches: the moss *PLDs*; Background branches: the clubmoss, liverwort, and fern *PLDs*.

**TABLE 2** The branch-site model test result for *CpPLD2* and *PpPLD11*.

Model	InL	2 $\Delta$ InL	Estimates of parameters	Positively selected sites
Model A	−29282.01	25.97 $p = 3.46 \times 10^{-7}$	$p0 = 0.75$ $p1 = 4.84 \times 10^{-3}$ ( $p2+p3 = 0.24$ ) $\omega 0 = 0.06$ $\omega 1 = 1.00$ $\omega 2 = 7.44$	188T (0.98) 225K (1.00) 227P (1.00) 234E (1.00) 238L (1.00) 242C (0.99)
Model A Null	−29295.00		$p0 = 0.62$ $p1 = 3.77 \times 10^{-3}$ ( $p2+p3 = 0.38$ ) $\omega 0 = 0.06$ $\omega 1 = 1.00$ $\omega 2 = 1.00$	262K (1.00) 263F (1.00) 265Y (0.99) 334K (1.00) 366R (1.00) 375Q (1.00)

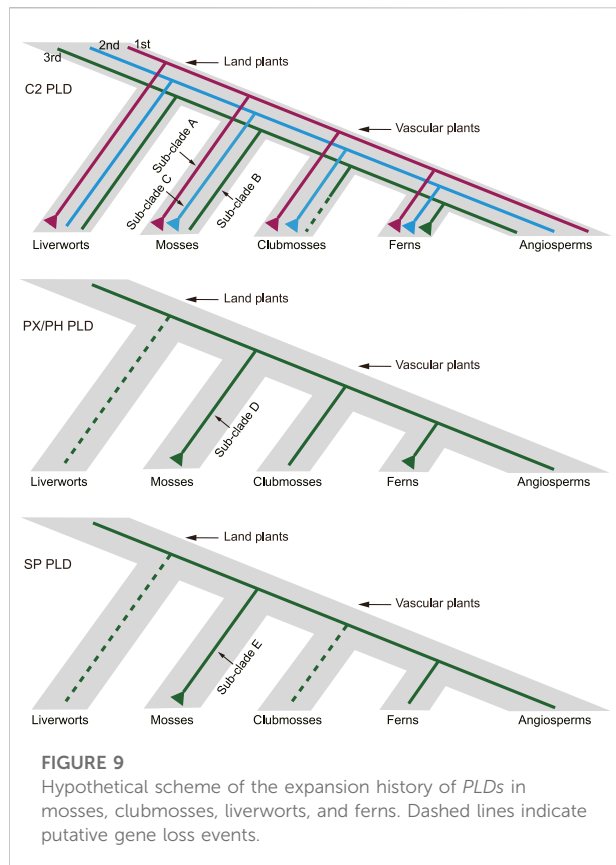
InL, log likelihood; 2 $\Delta$ InL, twice the log-likelihood difference between the two models. Positively selected sites were produced by Bayes Empirical Bayes analysis. Amino acids referred to *PpPLD11*.



homology modeling had a global model quality estimate (GMQE, a value between 0 and 1) of 0.77 (Supplementary Figure S6). On these two models, nine positively selected sites (188T, 225K, 227P, 234E, 238L, 262K, 263F, 265Y, and 334K) were present in the loop region, and three positively selected sites (242C, 366R, and 375Q) were distributed in the helix. Interestingly, these 12 positively selected sites were located on the surface of the 3D structures (Figure 8C and Supplementary Figure S6).

## Discussion

Despite that the *PLD* gene members have been widely documented in various angiosperms, such as *A. thaliana*, *Gossypium arboreum*, and *Camellia sinensis*, (Qin and Wang, 2002; Tang et al., 2016; Roshan et al., 2021), little is known about the diversification of moss *PLDs*. To fill this gap in our knowledge, we performed a genome-wide comparative analysis of *PLD* genes among six mosses, one clubmoss, one liverwort, and



three ferns. The 132 *PLDs* identified were not considered the result of sequencing contamination, because they were mapped to well-assembled scaffolds or chromosomes, and most of them were found to be expressed. However, it is still possible that several *PLD* genes (e.g., *M. polymorpha* *PLDs* 8–10) may suffer from genome assembly errors considering that their protein sequences are unusually short.

The phylogenetic analysis divided the plant *PLDs* into four distinct clades (I–IV), mostly consistent with the categorization of C2, PX/PH, and SP *PLDs*. Our results suggested that the origin of land plant C2, PX/PH, and SP *PLDs* could be traced back at least to the emergence of green algae. Furthermore, we reconstructed a hypothetical evolutionary pattern for moss *PLDs* (Figure 9). Three ancestral C2 *PLDs* (clades I and II, i.e.,  $\alpha$ ,  $\beta$ ,  $\gamma$ ,  $\epsilon$ , and  $\delta$  *PLDs*) were predicted to have diverged before the most recent common ancestor (MRCA) of land plants. The first and second ancestral C2 *PLD* copies (e.g., the homologs of the moss sub-clades A and C, respectively) were expanded in mosses. The rapid expansion of the first ancestral copy was also observed in all investigated liverworts, clubmosses, and ferns. The third ancestral C2 *PLD* copy (e.g., the homologs of the moss sub-clade B) was highly conserved in mosses, with exactly one homolog per species. For both PX/PH and SP *PLDs*, only one ancestral *PLD* was present in the MRCA of land plants. The primary expansion of moss PX/PH *PLD* had occurred before the splitting of the bryophyte lineage. Of note,

duplication of SP *PLD* was observed in *S. fallax* but not in other investigated mosses. The *S. fallax* SP *PLDs* are believed to emerge from one segmental duplication and four tandem duplications.

In *P. patens*, it was reported that two separate whole genome duplication (WGD) events occurred 27–35 and 40–48 million years ago (Lang et al., 2018). Here, we demonstrated that WGD greatly contributed to the recent *P. patens*-specific *PLD* duplications. This expansion pattern differed from the small-scale gene duplications (e.g., tandem and proximal gene duplications) that mainly occurred to *PLDs* of *S. fallax* and *C. purpureus*. For instance, *PpPLD2* and *PpPLD8* were located on chromosomes 8 and 23, respectively, and both *PpPLD6* and *PpPLD11* were anchored to chromosome 20. Together with the fact that chromosomes 8, 20, and 23 are derived from a common ancestor (Lang et al., 2018), it is likely that the primary WGD generated *PpPLD2* and the ancestor of *PpPLDs* 6, 8, and 11, and the second WGD yielded *PpPLD8* and the ancestor of *PpPLD6* and *PpPLD11*, with a subsequent tandem duplication on chromosome 20 producing the current *PpPLD6* and *PpPLD11*.

In the same *PLD* clade, the domains, motifs, and exons had similar arrangements, lending further support to the aforementioned classification of the four clades. The N-terminal C2 domain prevalent in clade I and II (i.e.,  $\alpha$ ,  $\beta$ ,  $\gamma$ ,  $\epsilon$ , and  $\delta$ ) *PLDs* is a  $\text{Ca}^{2+}$ -dependent phospholipid binding region critical for the affinity to substrates (Wang, 2005). The PX/PH domains specific to the clade III *PLDs* (*PLD* $\zeta$ s) are crucial to *PLD* phosphoinositide binding activity, subcellular distribution and intracellular trafficking (Morris, 2007). The HKD1 and HKD2 motifs can be packed against each other, forming the core structure essential for *PLD* catalysis (Li et al., 2020). Our work revealed that more than 82% of the *PLDs* identified in mosses, liverworts, clubmosses, and ferns contained certain clade-specific sequence similarities (the C2, PX/PH domains, or the signal peptide sequences), and over 95% shared the HKD1 or HKD2 motifs, implying high inter- and intra-clade genetic conservation. In addition, we found moss-specific intron removal in PX/PH ( $\zeta$ ) *PLDs*. Such intron losses may provide evolutionary advantages through expression regulation and functional differentiation (Park et al., 2010; Wang H. et al., 2014).

Identification of the drought, salt, low-temperature, wound, and anaerobic related *cis*-elements in the *PpPLD* promoter regions suggested that these genes are associated with *P. patens* response to various stresses. For example, the LTR *cis*-acting element was involved in low-temperature responsiveness (Brown et al., 2001). The wheat cytosolic glyceraldehyde-3-phosphate dehydrogenase 1 gene, which contained the LTR and MBS *cis*-acting elements in its promoters, showed an upregulated expression under salt stress (Fei et al., 2017). Our results also suggested that *PpPLDs* were likely related to light and phytohormone responses, and body development, through *cis*-elements such as Gap-box, ABRE, and CAT-box (Park et al., 1996; Choi et al., 2000).

RNA-seq based gene expression analysis revealed that most *PLDs* of mosses, clubmosses, ferns, and liverworts were expressed in transcriptome experiments. Among the *PLDs* of *P. patens* and

*C. purpureus*, *PpPLD3* and *CpPLD6* (both from moss sub-clade A, *PLDAs*) exhibited the most abundant expression, suggesting that in the experimental studies, the  $\alpha$  *PLDs* might provide important functions to these two closely related mosses. For *P. patens*, 12 of the 14 *PLDs* were expressed in different life cycle phases, implying a crucial role in plant growth and development. We also found that about half of the *P. patens* *PLD* genes responded to environmental stresses. In particular, four  $\alpha$  *PLDs*, i.e., *PpPLD2*, *PpPLD6*, *PpPLD10*, and *PpPLD11*, were involved in biotic and abiotic stress responses. These findings are expected given that *PLDAs* are known to function in stress-induced signaling in angiosperms (Kargiotidou et al., 2010; Bourtsala et al., 2017; Ufer et al., 2017).

A previous adaptive evolution analysis suggested that positive selection drove the evolution of PX/PH and SP *PLDs* of *Arabidopsis*, rice, poplar, and grape (Liu et al., 2010). In the present study, we found evidence that most of the C2, PX/PH, and SP *PLDs* of mosses, clubmosses, liverworts, and ferns were subject to ongoing purifying selection, indicating the dominance of non-synonymous mutations during the evolution of early land plant *PLD* gene family. In addition, both relaxed and intensified selections were found in moss C2 *PLDs*. These results suggested that the C2 *PLDs* were particularly diversified and might be a potential source of new biological functions during moss evolution. In support of this conclusion, the moss C2 *PLDs* were found to display highly diverse gene structures and were the most differentially expressed.

Mosses are considered one of the earliest colonizers of land. During their transition from aquatic to terrestrial habitat, mosses had to tolerate biotic and abiotic stresses such as viruses, drought and salinity (Yue et al., 2012). Intriguingly, our results obtained through multiple methods suggested that several sites and/or branches of clade I–IV *PLDs* (C2, PX/PH, and SP *PLDs*) experienced an episode of positive selection in the moss lineage. Among them, the strongest positive selection signals were detected in the moss C2 *PLDs*, e.g., *P. patens* *PLD11* and *C. purpureus* *PLD2*. The predicted three-dimensional model of *PpPLD11* revealed that the 12 positively selected sites existed on the enzyme's surface, suggesting that they may affect substrate binding ability. In angiosperms, C2 *PLDs* are implicated in response to diverse environmental stressors (Wang, 2005; Zhao, 2015). For example, overexpression of the heterologous C2 *PLDs* (*PLDAs*) in *Arabidopsis* and tobacco (*Nicotiana spp.*) improved the tolerance of these plants to drought and osmotic stress (Wang J. et al., 2014; Ji et al., 2017). We reason that the evolution of *PpPLDs* might confer beneficial traits particularly associated with stress regulatory networks, and thereby facilitated *P. patens* adaptation to terrestrial environments.

In summary, we revealed 84 *PLD* genes in six mosses, and investigated their evolutionary history. Conserved sequence characteristics (e.g., domain, motif, and gene structure), and expression of these *PLDs*, especially *P. patens* *PLDs* were examined. Although purifying selection largely drove the evolution of *PLDs* of mosses, liverworts, clubmosses, and ferns, episodic positive selection left footprints in the genetic diversity of moss *PLDs*. Our results will be

informative for designing experiments to better understand the biological functions of *PLDs* in mosses. Future exploration of *PLDs* from more different plant groups and deciphering their functions may help dissect the evolution of *PLD*-mediated signaling in plants.

## Data availability statement

The datasets presented in this study can be found in online repositories. The names of the repository/repositories and accession number(s) can be found in the article/Supplementary Material.

## Author contributions

ML and JZ conceived the study and wrote the manuscript. ML, JZ, XP, and WL participated in the data analysis. All authors approved the final version to be submitted for publication.

## Funding

This work was supported by a grant from the Yunnan Fundamental Research Projects (grant No. 202001AU070044) to ML and from the Yunnan University's Research Innovation Fund for Graduate Students (No. 2020Z80) to JZ.

## Acknowledgments

The authors thank Fengyi Hu for his helpful suggestions.

## Conflict of interest

The authors declare that the research was conducted in the absence of any commercial or financial relationships that could be construed as a potential conflict of interest.

## Publisher's note

All claims expressed in this article are solely those of the authors and do not necessarily represent those of their affiliated organizations, or those of the publisher, the editors and the reviewers. Any product that may be evaluated in this article, or claim that may be made by its manufacturer, is not guaranteed or endorsed by the publisher.

## Supplementary material

The Supplementary Material for this article can be found online at: <https://www.frontiersin.org/articles/10.3389/fgene.2022.1015393/full#supplementary-material>

## References

- Bailey, T. L., and Gribskov, M. (1998). Combining evidence using p-values: Application to sequence homology searches. *Bioinformatics* 14, 48–54. doi:10.1093/bioinformatics/14.1.48
- Beerling, D. J., Osborne, C. P., and Chaloner, W. G. (2001). Evolution of leaf-form in land plants linked to atmospheric CO<sub>2</sub> decline in the Late Palaeozoic era. *Nature* 410, 352–354. doi:10.1038/35066546
- Bourtsala, A., Farmaki, T., and Galanopoulou, D. (2017). Phospholipases Dα and δ are involved in local and systemic wound responses of cotton (*G. hirsutum*). *Biochem. Biophys. Rep.* 9, 133–139. doi:10.1016/j.bbrep.2016.12.001
- Boyce, C. K. (2008). How green was cooksonia? The importance of size in understanding the early evolution of physiology in the vascular plant lineage. *Paleobiology* 34, 179–194. doi:10.1666/0094-8373(2008)034[0179:Hgwcti]2.0.Co;2
- Bray, N. L., Pimentel, H., Melsted, P., and Pachter, L. (2016). Near-optimal probabilistic RNA-seq quantification. *Nat. Biotechnol.* 34, 525–527. doi:10.1038/nbt.3519
- Brown, A. P. C., Dunn, M. A., Goddard, N. J., and Hughes, M. A. (2001). Identification of a novel low-temperature-response element in the promoter of the barley (*Hordeum vulgare* L) gene *blt101.1*. *Planta* 213, 770–780. doi:10.1007/s004250100549
- Brown, D. M., Zeef, L. a. H., Ellis, J., Goodacre, R., and Turner, S. R. (2005). Identification of novel genes in *Arabidopsis* involved in secondary cell wall formation using expression profiling and reverse genetics. *Plant Cell* 17, 2281–2295. doi:10.1105/tpc.105.031542
- Camacho, C., Coulouris, G., Avagyan, V., Ma, N., Papadopoulos, J., Bealer, K., et al. (2009). BLAST+: Architecture and applications. *BMC Bioinforma.* 10, 421. doi:10.1186/1471-2105-10-421
- Capella-Gutierrez, S., Silla-Martinez, J. M., and Gabaldon, T. (2009). trimAl: a tool for automated alignment trimming in large-scale phylogenetic analyses. *Bioinformatics* 25, 1972–1973. doi:10.1093/bioinformatics/btp348
- Choi, H.-I., Hong, J.-H., Ha, J.-O., Kang, J.-Y., and Kim, S. Y. (2000). ABFs, a family of ABA-responsive element binding factors. *J. Biol. Chem.* 275, 1723–1730. doi:10.1074/jbc.275.3.1723
- Elias, M., Potocky, M., Cvrckova, F., and Zarsky, V. (2002). Molecular diversity of phospholipase D in angiosperms. *BMC Genomics* 3, 2. doi:10.1186/1471-2164-3-2
- Fei, Y., Xue, Y., Du, P., Yang, S., and Deng, X. (2017). Expression analysis and promoter methylation under osmotic and salinity stress of *TaGAPC1* in wheat (*Triticum aestivum* L). *Protoplasma* 254, 987–996. doi:10.1007/s00709-016-1008-5
- Finn, R. D., Bateman, A., Clements, J., Coggill, P., Eberhardt, R. Y., Eddy, S. R., et al. (2013). Pfam: The protein families database. *Nucleic Acids Res.* 42, D222–D230. doi:10.1093/nar/gkt1223
- Fisher, R. A. (1992). “Statistical methods for research workers,” in *Breakthroughs in statistics: Methodology and distribution*. Editors S. Kotz and N. L. Johnson (New York, NY: Springer New York), 66–70. doi:10.1007/978-1-4612-4380-9\_6
- Hansen, B. O., Vaid, N., Musialak-Lange, M., Janowski, M., and Mutwil, M. (2014). Elucidating gene function and function evolution through comparison of co-expression networks of plants. *Front. Plant Sci.* 5, 394. doi:10.3389/fpls.2014.00394
- Harris, B. J., Harrison, C. J., Hetherington, A. M., and Williams, T. A. (2020). Phylogenomic evidence for the monophyly of bryophytes and the reductive evolution of stomata. *Curr. Biol.* 30, 2001–2012. doi:10.1016/j.cub.2020.03.048
- Hong, Y., Pan, X., Welti, R., and Wang, X. (2008). Phospholipase Dα3 is involved in the hyperosmotic response in *Arabidopsis*. *Plant Cell* 20, 803–816. doi:10.1105/tpc.107.056390
- Hong, Y., Devaiah, S. P., Bahn, S. C., Thamasandra, B. N., Li, M., Welti, R., et al. (2009). Phospholipase D epsilon and phosphatidic acid enhance *Arabidopsis* nitrogen signaling and growth. *Plant J.* 58, 376–387. doi:10.1111/j.1365-313X.2009.03788.x
- Hong, K., Zhang, L., Zhan, R., Huang, B., Song, K., and Jia, Z. (2017). Identification and characterization of phospholipase D genes putatively involved in internal browning of pineapple during postharvest storage. *Front. Plant Sci.* 8, 913. doi:10.3389/fpls.2017.00913
- Jang, J. H., Lee, C. S., Hwang, D., and Ryu, S. H. (2012). Understanding of the roles of phospholipase D and phosphatidic acid through their binding partners. *Prog. Lipid Res.* 51, 71–81. doi:10.1016/j.plipres.2011.12.003
- Ji, T., Li, S., Huang, M., Di, Q., Wang, X., Wei, M., et al. (2017). Overexpression of cucumber phospholipase D alpha gene (*CsPLDa*) in tobacco enhanced salinity stress tolerance by regulating Na<sup>+</sup>-K<sup>+</sup> balance and lipid peroxidation. *Front. Plant Sci.* 8, 499. doi:10.3389/fpls.2017.00499
- Jumper, J., Evans, R., Pritzel, A., Green, T., Figurnov, M., Ronneberger, O., et al. (2021). Highly accurate protein structure prediction with AlphaFold. *Nature* 596, 583–589. doi:10.1038/s41586-021-03819-2
- Kargiotidou, A., Kappas, I., Tsafaris, A., Galanopoulou, D., and Farmaki, T. (2010). Cold acclimation and low temperature resistance in cotton: *Gossypium hirsutum* phospholipase alpha isoforms are differentially regulated by temperature and light. *J. Exp. Bot.* 61, 2991–3002. doi:10.1093/jxb/erq124
- Katoh, K., and Standley, D. M. (2013). MAFFT multiple sequence alignment software version 7: Improvements in performance and usability. *Mol. Biol. Evol.* 30, 772–780. doi:10.1093/molbev/mst010
- Kopka, J., Pical, C., Hetherington, A. M., and Muller-Rober, B. (1998). Ca<sup>2+</sup>/phospholipid-binding (C<sub>2</sub>) domain in multiple plant proteins: Novel components of the calcium-sensing apparatus. *Plant Mol. Biol.* 36, 627–637. doi:10.1023/a:1005915020760
- Kosakovsky Pond, S. L., Poon, A. F. Y., Velazquez, R., Weaver, S., Hepler, N. L., Murrell, B., et al. (2020). HyPhy 2.5—A customizable platform for evolutionary hypothesis testing using phylogenies. *Mol. Biol. Evol.* 37, 295–299. doi:10.1093/molbev/msz197
- Lang, D., Ullrich, K. K., Murat, F., Fuchs, J., Jenkins, J., Haas, F. B., et al. (2018). The *Physcomitrella patens* chromosome-scale assembly reveals moss genome structure and evolution. *Plant J.* 93, 515–533. doi:10.1111/tpj.13801
- Letunic, I., Khedkar, S., and Bork, P. (2020). Smart: Recent updates, new developments and status in 2020. *Nucleic Acids Res.* 49, D458–D460. doi:10.1093/nar/gkaa937
- Li, F.-W., Brouwer, P., Carretero-Paulet, L., Cheng, S., De Vries, J., Delaux, P.-M., et al. (2018). Fern genomes elucidate land plant evolution and cyanobacterial symbioses. *Nat. Plants* 4, 460–472. doi:10.1038/s41477-018-0188-8
- Li, J., Yu, F., Guo, H., Xiong, R., Zhang, W., He, F., et al. (2020). Crystal structure of plant PLDα1 reveals catalytic and regulatory mechanisms of eukaryotic phospholipase D. *Cell Res.* 30, 61–69. doi:10.1038/s41422-019-0244-6
- Li, L., Zhang, C., Zhang, M., Yang, C., Bao, Y., Wang, D., et al. (2021). Genome-wide analysis and expression profiling of the phospholipase D gene family in *Solanum tuberosum*. *Biology* 10, 741. doi:10.3390/biology10080741
- Liu, Q., Zhang, C., Yang, Y., and Hu, X. (2010). Genome-wide and molecular evolution analyses of the phospholipase D gene family in Poplar and Grape. *BMC Plant Biol.* 10, 117. doi:10.1186/1471-2229-10-117
- Liu, S.-L., Zhuang, Y., Zhang, P., and Adams, K. L. (2009). Comparative analysis of structural diversity and sequence evolution in plant mitochondrial genes transferred to the nucleus. *Mol. Biol. Evol.* 26, 875–891. doi:10.1093/molbev/msp011
- Mane, S. P., Vasquez-Robinet, C., Sioson, A. A., Heath, L. S., and Grene, R. (2007). Early PLDα-mediated events in response to progressive drought stress in *Arabidopsis*: A transcriptome analysis. *J. Exp. Bot.* 58, 241–252. doi:10.1093/jxb/erl262
- Morris, A. J. (2007). Regulation of phospholipase D activity, membrane targeting and intracellular trafficking by phosphoinositides. *Biochem. Soc. Symp.* 74, 247–257. doi:10.1042/BSS0740247
- Murrell, B., Moola, S., Mabona, A., Weighill, T., Sheward, D., Kosakovsky Pond, S. L., et al. (2013). Fubar: A fast, unconstrained bayesian approximation for inferring selection. *Mol. Biol. Evol.* 30, 1196–1205. doi:10.1093/molbev/mst030
- Murrell, B., Weaver, S., Smith, M. D., Wertheim, J. O., Murrell, S., Aylward, A., et al. (2015). Gene-wide identification of episodic selection. *Mol. Biol. Evol.* 32, 1365–1371. doi:10.1093/molbev/msv035
- Murrell, B., Wertheim, J. O., Moola, S., Weighill, T., Scheffler, K., and Kosakovsky Pond, S. L. (2012). Detecting individual sites subject to episodic diversifying selection. *PLoS Genet.* 8, e1002764. doi:10.1371/journal.pgen.1002764
- Nguyen, L. T., Schmidt, H. A., Von Haeseler, A., and Minh, B. Q. (2015). IQ-TREE: A fast and effective stochastic algorithm for estimating maximum-likelihood phylogenies. *Mol. Biol. Evol.* 32, 268–274. doi:10.1093/molbev/msu300
- Nielsen, H. (2017). “Predicting secretory proteins with SignalP,” in *Protein function prediction: Methods and protocols*. Editor D. Kihara (New York, NY: Springer New York), 59–73. doi:10.1007/978-1-4939-7015-5\_6
- Ortiz-Ramirez, C., Hernandez-Coronado, M., Thamm, A., Catarino, B., Wang, M., Dolan, L., et al. (2016). A transcriptome atlas of *Physcomitrella patens* provides insights into the evolution and development of land plants. *Mol. Plant* 9, 205–220. doi:10.1016/j.molp.2015.12.002
- Park, S. C., Kwon, H. B., and Shih, M. C. (1996). Cis-acting elements essential for light regulation of the nuclear gene encoding the A subunit of chloroplast

- glyceraldehyde 3-phosphate dehydrogenase in *Arabidopsis thaliana*. *Plant Physiol.* 112, 1563–1571. doi:10.1104/pp.112.4.1563
- Park, K.-C., Kwon, S.-J., and Kim, N.-S. (2010). Intron loss mediated structural dynamics and functional differentiation of the polygalacturonase gene family in land plants. *Genes Genomics* 32, 570–577. doi:10.1007/s13258-010-0076-8
- Pederson, E. R. A., Warshan, D., and Rasmussen, U. (2019). Genome sequencing of *Pleurozium schreberi*: The assembled and annotated draft genome of a pleurocarpous feather moss. *G3* 9, 2791–2797. doi:10.1534/g3.119.400279
- Pichersky, E., and Gang, D. R. (2000). Genetics and biochemistry of secondary metabolites in plants: An evolutionary perspective. *Trends Plant Sci.* 5, 439–445. doi:10.1016/S1360-1385(00)01741-6
- Pinosa, F., Buhot, N., Kwaaitaal, M., Fahlberg, P., Thordal-Christensen, H., Ellerström, M., et al. (2013). *Arabidopsis* phospholipase D $\delta$  is involved in basal defense and nonhost resistance to powdery mildew fungi. *Plant Physiol.* 163, 896–906. doi:10.1104/pp.113.223503
- Qin, C., and Wang, X. (2002). The *Arabidopsis* phospholipase D family. Characterization of a calcium-independent and phosphatidylcholine-selective PLD zeta 1 with distinct regulatory domains. *Plant Physiol.* 128, 1057–1068. doi:10.1104/pp.010928
- Qu, L., Chu, Y.-J., Lin, W.-H., and Xue, H.-W. (2021). A secretory phospholipase D hydrolyzes phosphatidylcholine to suppress rice heading time. *PLoS Genet.* 17, e1009905. doi:10.1371/journal.pgen.1009905
- Ranwez, V., Douzery, E. J. P., Cambon, C., Chantret, N., and Delsuc, F. (2018). MACSE v2: Toolkit for the alignment of coding sequences accounting for frameshifts and stop codons. *Mol. Biol. Evol.* 35, 2582–2584. doi:10.1093/molbev/msy159
- Ronquist, F., Teslenko, M., Van Der Mark, P., Ayres, D. L., Darling, A., Höhna, S., et al. (2012). MrBayes 3.2: Efficient bayesian phylogenetic inference and model choice across a large model space. *Syst. Biol.* 61, 539–542. doi:10.1093/sysbio/sys029
- Roshan, N. M., Ashouri, M., and Sadeghi, S. M. (2021). Identification, evolution, expression analysis of phospholipase D (PLD) gene family in tea (*Camellia sinensis*). *Physiol. Mol. Biol. Plants.* 27, 1219–1232. doi:10.1007/s12298-021-01007-0
- Ryu, S. B., Zheng, L., and Wang, X. (1996). Changes in phospholipase D expression in soybeans during seed development and germination. *J. Am. Oil Chem. Soc.* 73, 1171–1176. doi:10.1007/BF02523380
- Selvy, P. E., Lavieri, R. R., Lindsley, C. W., and Brown, H. A. (2011). Phospholipase D: Enzymology, functionality, and chemical modulation. *Chem. Rev.* 111, 6064–6119. doi:10.1021/cr200296t
- Singh, A., Pandey, A., Baranwal, V., Kapoor, S., and Pandey, G. K. (2012). Comprehensive expression analysis of rice phospholipase D gene family during abiotic stresses and development. *Plant Signal. Behav.* 7, 847–855. doi:10.4161/psb.20385
- Smith, M. D., Wertheim, J. O., Weaver, S., Murrell, B., Scheffler, K., and Kosakovsky Pond, S. L. (2015). Less is more: An adaptive branch-site random effects model for efficient detection of episodic diversifying selection. *Mol. Biol. Evol.* 32, 1342–1353. doi:10.1093/molbev/msv022
- Tang, K., Dong, C., and Liu, J. (2016). Genome-wide analysis and expression profiling of the phospholipase D gene family in *Gossypium arboreum*. *Sci. China. Life Sci.* 59, 130–141. doi:10.1007/s11427-015-4916-2
- Ufer, G., Gertzmann, A., Gasulla, F., Röhrig, H., and Bartels, D. (2017). Identification and characterization of the phosphatidic acid binding *A. thaliana* phosphoprotein PLDrp1 which is regulated by PLDa1 in a stress dependent manner. *Plant J.* 92, 276–290. doi:10.1111/tipj.13651
- Wang, H., Devos, K. M., and Bennetzen, J. L. (2014a). Recurrent loss of specific introns during angiosperm evolution. *PLoS Genet.* 10, e1004843. doi:10.1371/journal.pgen.1004843
- Wang, J., Ding, B., Guo, Y., Li, M., Chen, S., Huang, G., et al. (2014b). Overexpression of a wheat phospholipase D gene, *TaPLDa*, enhances tolerance to drought and osmotic stress in *Arabidopsis thaliana*. *Planta* 240, 103–115. doi:10.1007/s00425-014-2066-6
- Wang, X. (2000). Multiple forms of phospholipase D in plants: The gene family, catalytic and regulatory properties, and cellular functions. *Prog. Lipid Res.* 39, 109–149. doi:10.1016/s0163-7827(00)00002-3
- Wang, X. (2005). Regulatory functions of phospholipase D and phosphatidic acid in plant growth, development, and stress responses. *Plant Physiol.* 139, 566–573. doi:10.1104/pp.105.068809
- Waterhouse, A., Bertoni, M., Bienert, S., Studer, G., Tauriello, G., Gumienny, R., et al. (2018). SWISS-MODEL: Homology modelling of protein structures and complexes. *Nucleic Acids Res.* 46, W296–W303. doi:10.1093/nar/gky427
- Wertheim, J. O., Murrell, B., Smith, M. D., Kosakovsky Pond, S. L., and Scheffler, K. (2015). Relax: Detecting relaxed selection in a phylogenetic framework. *Mol. Biol. Evol.* 32, 820–832. doi:10.1093/molbev/msu400
- Yang, Z. (2007). Paml 4: Phylogenetic analysis by maximum likelihood. *Mol. Biol. Evol.* 24, 1586–1591. doi:10.1093/molbev/msm088
- Yu, J., Li, L., Wang, S., Dong, S., Chen, Z., Patel, N., et al. (2020). Draft genome of the aquatic moss *Fontinalis antipyretica* (Fontinalaceae, Bryophyta). *Gigabyte*, 1–9. doi:10.46471/gigabyte.8
- Yue, J., Hu, X., Sun, H., Yang, Y., and Huang, J. (2012). Widespread impact of horizontal gene transfer on plant colonization of land. *Nat. Commun.* 3, 1152. doi:10.1038/ncomms2148
- Zhang, W., Wan, X., Hong, Y., Li, W., and Wang, X. (2010). “Plant phospholipase D,” in *Lipid signaling in plants*. Editor T. Munnik (Berlin: Springer), 39–62. doi:10.1007/978-3-642-03873-0\_3
- Zhao, J. (2015). Phospholipase D and phosphatidic acid in plant defence response: From protein-protein and lipid-protein interactions to hormone signalling. *J. Exp. Bot.* 66, 1721–1736. doi:10.1093/jxb/eru540